

Dipole polarizability of ${}^6\text{He}$ and its effect on elastic scattering

K. Rusek*

Department of Nuclear Reactions, The Andrzej Sothan Institute for Nuclear Studies, Hoza 69, PL-00-681 Warsaw, Poland

N. Keeley and K. W. Kemper

Physics Department, Florida State University, Tallahassee, Florida 32306-4350

R. Raabe†

*Instituut voor Kern- en Stralingsfysica, Katholieke Universiteit Leuven, B-3001 Leuven, Belgium
and DSM/DAPNIA CEA Saclay, F-91191 Gif-sur-Yvette, France*

(Received 16 January 2003; published 28 April 2003)

The elastic scattering of ${}^6\text{Li}$ and ${}^6\text{He}$ by ${}^{208}\text{Pb}$ at energies in the vicinity of the Coulomb barrier is studied by means of continuum-discretized coupled-channels calculations. It is shown that the strong reduction of the ${}^6\text{He}+{}^{208}\text{Pb}$ elastic scattering cross section at forward angles is caused by long-range dipole Coulomb excitation of the projectile. The role of breakup in the fusion of halo nuclei is also discussed.

DOI: 10.1103/PhysRevC.67.041604

PACS number(s): 21.60.Gx, 24.10.Eq, 25.70.Bc, 25.70.De

It is expected that the dipole excitation of ${}^6\text{He}$ in the field of a highly charged nucleus should proceed with a large probability. This excitation mode occurs because the two halo neutrons are well separated from the charged core and the center of charge and the center of mass of the ${}^6\text{He}$ nucleus do not coincide. For energies in the vicinity of the Coulomb barrier, the dipole excitation is dominated by the long-range Coulomb force. For nuclei with a low breakup threshold, the effect of projectile excitation is to lower the elastic scattering cross section at small angles, and so the $E1$ excitation of ${}^6\text{He}$ should be observable as a reduction of the elastic scattering cross section. This consequence of its dipole polarizability was first predicted for scattering of the halo nucleus ${}^{11}\text{Li}$ from ${}^{208}\text{Pb}$ by Andrés *et al.* [1]. Coupled-channels calculations performed by Sakuragi *et al.* [2] confirmed this effect.

One very good opportunity to observe the effect of the dipole polarizability of ${}^6\text{He}$ is to compare its elastic scattering from a heavy target with that of the ${}^6\text{Li}$ nucleus, whose dipole polarizability should be very small. The two-body cluster model of Buck and Pilt [3] gives dipole reduced transition probabilities $B(E1)$ identically equal to zero for an $\alpha+d$ cluster. As ${}^6\text{Li}$ is very well described by such a cluster picture, any residual dipole polarizability in ${}^6\text{Li}$ will be very weak. Therefore, a comparison of similar experimental data for both nuclei, e.g., elastic scattering cross sections, should reveal any differences caused by the strong ${}^6\text{He}$ dipole polarizability. Both nuclei are of similar size and the binding energy of ${}^6\text{Li}$ is only slightly larger than that of ${}^6\text{He}$. While ${}^6\text{Li}$ has a well developed $\alpha+d$ cluster structure and ${}^6\text{He}$ is a three-body $\alpha+n+n$ object, the three-body wave function of the ${}^6\text{He}$ ground state has a dineutron (2n) component that dominates the tail of this wave function [4], giving rise to an $\alpha+{}^2n$ cluster structure. Because low energy ${}^6\text{He}$ scattering by a heavy target is only sensitive to the tail of the ${}^6\text{He}$ ground state wave function, the dineutron component should

be the dominant feature of this wave function. Therefore, one would expect that the two-body dineutron model of ${}^6\text{He}$ should account for most of the effects observed in such scattering.

There are many scattering datasets available for ${}^6\text{Li}$ but very few for ${}^6\text{He}$. At present, the only available elastic scattering data for ${}^6\text{He}$ by a heavy target at near-barrier energies are the ${}^6\text{He}+{}^{209}\text{Bi}$ data of Aguilera *et al.* [5], which are insufficiently accurate at forward angles to test the effect of dipole polarizability. Recently, however, ${}^6\text{He}$ elastic scattering by ${}^{208}\text{Pb}$ was measured at the Cyclotron Research Centre in Louvain-la-Neuve at an incident energy of 29.6 MeV. The experiment was part of a campaign (by the PH-114 Collaboration [6]) in which the elastic scattering of ${}^6\text{He}$ by different targets was investigated; details are given in Ref. [7]. The ${}^6\text{He}+{}^{208}\text{Pb}$ data are shown in Fig. 1 as the open circles. The angular distribution of the elastic scattering cross section (ratio to Rutherford cross section) does not exhibit a Coulomb rainbow, in contrast to the ${}^6\text{Li}+{}^{208}\text{Pb}$ scattering at a similar energy relative to the Coulomb barrier. In order to account for the different Coulomb barriers of the ${}^6\text{He}+{}^{208}\text{Pb}$ and ${}^6\text{Li}+{}^{208}\text{Pb}$ systems, we have compared elastic scattering data where the ratio of the c.m. energy to the nominal Coulomb-barrier energy, $E_{\text{c.m.}}/E_C$, is approximately the same. The nominal Coulomb-barrier energy was taken to be 20.75 MeV for ${}^6\text{He}+{}^{208}\text{Pb}$ and 31.13 MeV for ${}^6\text{Li}+{}^{208}\text{Pb}$.

In a recent publication [9], we have shown by means of continuum-discretized coupled-channels (CDCC) calculations that the absence of a distinct Coulomb rainbow for ${}^7\text{Be}+{}^{208}\text{Pb}$ scattering is caused by the low breakup threshold of the projectile. Based on this conclusion, we would predict that ${}^6\text{He}$, with an $\alpha+2n$ breakup threshold lower than the $\alpha+{}^3\text{He}$ one of ${}^7\text{Be}$, should have elastic scattering angular distributions for near-barrier energies from a heavy target such as ${}^{208}\text{Pb}$ which show a lack of a Coulomb rainbow. In this paper we present the results of CDCC calculations for ${}^6\text{He}+{}^{208}\text{Pb}$ and ${}^6\text{Li}+{}^{208}\text{Pb}$ in order to test whether this conclusion is supported by detailed model calculations.

The present CDCC calculations for ${}^6\text{Li}$, which include couplings to the resonant and nonresonant excited states of

*Electronic address: rusek@fuw.edu.pl

†For the PH-114 Collaboration.

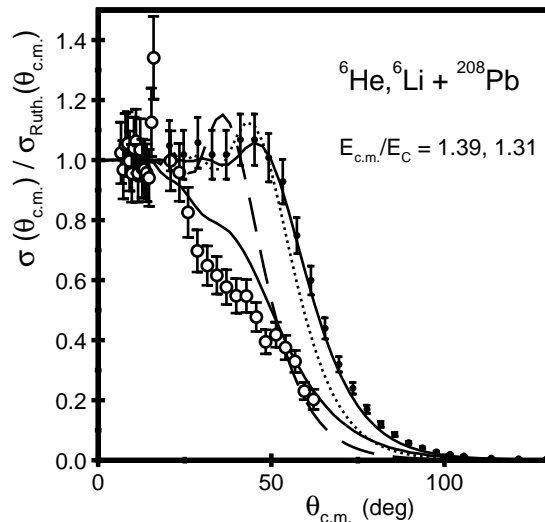


FIG. 1. Comparison of the angular distributions of the differential cross section (ratio to Rutherford cross section) for elastic scattering of ${}^6\text{He}$ (open circles) and ${}^6\text{Li}$ (filled circles) by a ${}^{208}\text{Pb}$ target. In order to account for the different Coulomb barriers the data are compared at similar values of the ratio of c.m. energy to the nominal Coulomb barrier energy, 1.39 for ${}^6\text{He}$ and 1.31 for ${}^6\text{Li}$. Experimental data are from Refs. [7,8]. Solid curves show the results of the full CDCC calculations while the dotted and dashed curves show the results of one-channel calculations for ${}^6\text{Li}$ and ${}^6\text{He}$, respectively. Note the linear cross section scale.

this nucleus, are only slightly modified in comparison with the calculations performed previously for ${}^6\text{Li}+{}^{208}\text{Pb}$ breakup [10]. The discretization of the $\alpha+d$ continuum was slightly changed and also the depths of the $\alpha+d$ binding potentials for the $L=2$ nonresonant states were taken to be the same as the depths of the potentials for the corresponding resonances. The input $\alpha+{}^{208}\text{Pb}$ and $d+{}^{208}\text{Pb}$ optical model potentials are the same as in Ref. [10].

For ${}^6\text{He}$, the dineutron model of Ref. [11] was assumed, with the continuum truncated at momentum $k=0.85\text{ fm}^{-1}$. The input $\alpha+{}^{208}\text{Pb}$ and dineutron+ ${}^{208}\text{Pb}$ optical model potentials were taken to be the same as the corresponding potentials used for ${}^6\text{Li}$. The potential binding the dineutron cluster to the α core used the set II parameters of Rusek *et al.* [11]. The coupled equations were integrated up to $R=260\text{ fm}$ for the lowest laboratory energy of 19 MeV. Calculations at a still lower energy would require a much larger model space and therefore were not performed. For the highest energy of 143.4 MeV the integration was carried out up to $R=35\text{ fm}$. The calculations were performed by means of the code FRESKO, version FRXP.18 [12].

In Fig. 1 the results of the CDCC calculations for ${}^6\text{Li}+{}^{208}\text{Pb}$ elastic scattering at a laboratory energy of 42 MeV and for ${}^6\text{He}+{}^{208}\text{Pb}$ at an energy of 29.6 MeV are plotted by the solid curves. The calculation for ${}^6\text{Li}$ fits very well the experimental data of Gemmeke *et al.* [8]. The dotted curve shows the result of a one-channel calculation which does not include breakup effects. Inclusion of the projectile breakup by means of the CDCC method damps the rainbow oscillations and, at larger scattering angles, enhances the elastic

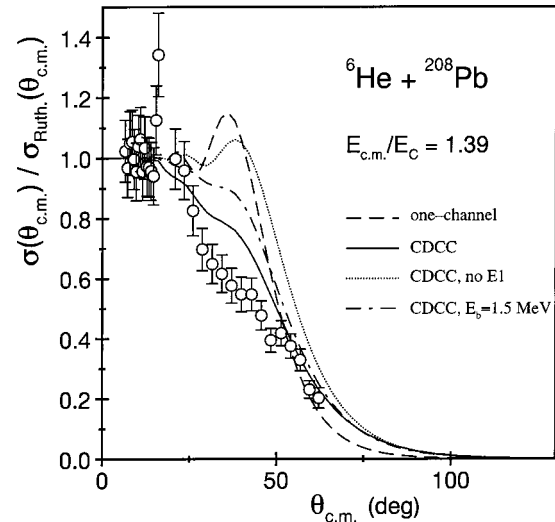


FIG. 2. Angular distribution of the differential cross section (ratio to Rutherford cross section) for ${}^6\text{He}+{}^{208}\text{Pb}$ elastic scattering. The solid and dashed curves show the results of calculations as in Fig. 1. The dotted curve corresponds to a CDCC calculation with $E1$ excitations switched off. The result of a CDCC calculation with the binding energy of ${}^6\text{He}$ increased to 1.5 MeV is indicated by the dot-dashed curve.

scattering cross section in a way similar to a reduction of the real part of the optical potential. For ${}^6\text{He}$, the difference between the one-channel calculation plotted as the dashed curve and the CDCC calculation shows a very large effect from ${}^6\text{He}$ breakup, which, at scattering angles larger than 50° , has the same nature as for ${}^6\text{Li}$. However, at more forward angles, the effect is much larger than that for ${}^6\text{Li}$. It damps completely the rainbow oscillations and considerably reduces the elastic scattering cross section. This is similar to the effect of an increase in the imaginary part of the optical potential.

The origin of this strong reduction was investigated in a series of test calculations. The results are presented in Fig. 2. When the $E1$ excitations were omitted from the coupling scheme, the effect of the ${}^6\text{He}$ breakup was similar to that for ${}^6\text{Li}$. The dotted curve in Fig. 2 represents the result of a CDCC calculation without $E1$ excitations. Clearly, the origin of the large reduction of the elastic scattering cross section can be attributed to the dipole polarizability of ${}^6\text{He}$. The fact that the ${}^6\text{He}$ nucleus is very weakly bound makes this effect larger. The dot-dashed curve shows the result of a CDCC calculation with the binding energy of ${}^6\text{He}$ increased to that of ${}^6\text{Li}$. In the latter case, the effect of the dipole polarizability is reduced but it is still large.

A comparison with the experimental data for the ${}^6\text{He}+{}^{208}\text{Pb}$ breakup would provide an important test of our CDCC calculations. Currently such data are not available. The two-neutron removal cross section for this scattering system was recently measured by Wang *et al.* [13] at a laboratory energy of 143.4 MeV. Although the dineutron model used by us may not work well at this high energy, we decided to perform a test calculation. The measured value for the two-neutron removal cross section was $1700\pm 100\text{ mb}$

while the CDCC calculation gave 1130 mb for the ${}^6\text{He} \rightarrow \alpha + {}^2n$ breakup. Taking into account the possible shortcomings of the dineutron model and that processes other than the direct ${}^6\text{He}$ breakup can contribute to the measured cross section, this agreement is quite reasonable. The calculated total reaction cross section was 4940 mb while the measured value by Warner *et al.* [14] was 4510 ± 100 mb in the laboratory energy range 138–378 MeV.

There is a long-running discussion as to how breakup affects the fusion cross section of weakly bound nuclei. It was shown [15] that the breakup process can be simulated in one-channel calculations by a repulsive polarization potential, which, for heavy targets, may enhance the elastic scattering cross section and lead to the reduction of the fusion cross section. On the other hand, there are suggestions [16] that in the case of halo nuclei the breakup effectively reduces the barrier and leads to the enhancement of the fusion cross section. Experimentally, the suppression of the fusion cross section due to breakup was reported recently for ${}^6,7\text{Li} + {}^{209}\text{Bi}$ by Dasgupta *et al.* [17], while Kolata *et al.* [18] observed a large enhancement of the ${}^6\text{He} + {}^{209}\text{Bi}$ fusion cross section at sub-barrier energies in comparison with model calculations. This enhancement was also reported for ${}^6\text{He} + {}^{238}\text{U}$ by Trotta *et al.* [19].

The mechanisms of the ${}^6\text{Li}$ and ${}^6\text{He}$ breakups in the field of a lead target are different. The breakup of ${}^6\text{He}$ is dominated by $E1$ transitions to the continuum while ${}^6\text{Li}$ breaks up into $\alpha + d$ by means of quadrupole couplings to the resonant and nonresonant states. These quadrupole couplings are driven mainly by nuclear forces. Therefore, the breakup cross section for ${}^6\text{He}$ is much larger than the breakup cross section for ${}^6\text{Li}$. Thus, a comparison of the fusion cross sections for the ${}^6\text{Li} + {}^{208}\text{Pb}$ and ${}^6\text{He} + {}^{208}\text{Pb}$ systems should provide some information on the role of breakup in the fusion process. On the other hand, ${}^6\text{Li}$ and ${}^6\text{He}$ differ in binding energies and this difference may also influence the fusion cross section. In order to investigate fusion, we have performed CDCC calculations for both scattering systems at a few energies around the Coulomb barrier. The fusion cross section was extracted from the CDCC calculations using the method described in our previous paper [9]. From the CDCC calculations an effective potential (bare plus polarization potential) was obtained for each of the investigated systems. This effective potential was then used to calculate the fusion cross section by means of the barrier penetration model. The results are presented in Fig. 3.

At present, no experimental data are available for the fusion of ${}^6\text{Li}$ or ${}^6\text{He}$ with ${}^{208}\text{Pb}$ around the barrier. However, for ${}^6\text{He}$ there is a dataset for the neighboring target ${}^{209}\text{Bi}$ [18] and these data are plotted in Fig. 3. The dashed and dot-dashed curves show the results of calculations for ${}^6\text{He}$ and for ${}^6\text{Li}$, respectively, with the breakup couplings omitted. The difference between the calculated fusion cross sections for both projectiles can be attributed to their different binding energies or to the halo structure of ${}^6\text{He}$. However, when the breakup couplings were included, this large difference was canceled by the breakup effects. The fusion cross sections were reduced, as shown by the solid (for ${}^6\text{He}$) and

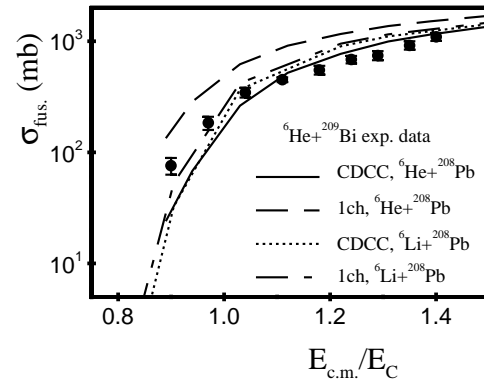


FIG. 3. Comparison of the calculated fusion cross section for ${}^6\text{He} + {}^{208}\text{Pb}$ with the experimental data measured by Kolata *et al.* [18] for a ${}^{209}\text{Bi}$ target. The results of the CDCC calculations are plotted by the solid curve while the results of the one-channel calculations are plotted by the dashed curve, as in Figs. 1 and 2. Dotted and dot-dashed curves show the results of CDCC and one-channel calculations, respectively, for ${}^6\text{Li} + {}^{208}\text{Pb}$.

dotted (for ${}^6\text{Li}$) curves, and this reduction was much larger for ${}^6\text{He}$ than for ${}^6\text{Li}$. As a result, the calculated fusion cross sections for both projectiles are very similar, reflecting their similar sizes. Above the barrier the cross section for the more strongly bound nucleus ${}^6\text{Li}$ is slightly larger while below the barrier the cross section for the more loosely bound ${}^6\text{He}$ becomes larger. We have observed a very similar effect in our previous comparative studies of the ${}^7\text{Li}$, ${}^7\text{Be} + {}^{208}\text{Pb}$ systems [9].

In summary, we have performed realistic CDCC calculations for ${}^6\text{Li}$ and ${}^6\text{He}$ scattered by ${}^{208}\text{Pb}$ at energies around the Coulomb barrier. The calculations reproduced well the angular distributions of the differential cross section for elastic scattering. We have shown that the large reduction of the differential cross section for ${}^6\text{He} + {}^{208}\text{Pb}$ elastic scattering at forward angles is caused by the large dipole polarizability of the halo nucleus in the Coulomb field of the heavy target. Dipole excitation to the continuum is the dominant influence on the elastic scattering of ${}^6\text{He}$ by ${}^{208}\text{Pb}$, and the low ${}^6\text{He} \rightarrow \alpha + {}^2n$ threshold energy enhances this effect. For the fusion, the effect of breakup cancels the differences arising from the different binding energies and the calculated fusion cross sections for ${}^6\text{He}$ and ${}^6\text{Li}$ with a lead target are very similar. Our results suggest that the effect of the ${}^6\text{He}$ dipole polarizability could be seen in the fusion cross section below the barrier, when compared with the fusion cross section for ${}^6\text{Li}$ on the same target. In order to study these effects in more detail, we propose a series of experiments to measure accurate elastic scattering angular distributions for ${}^6\text{He} + {}^{208}\text{Pb}$ at energies in the vicinity of the Coulomb barrier as well as fusion cross sections for both projectiles with a lead target.

The authors thank Professor J. J. Kolata for providing numerical values of the ${}^6\text{He} + {}^{209}\text{Bi}$ fusion cross section. This work was financially supported by the State Committee for Scientific Research of Poland (KBN), POLONIUM Grant No. 4335.I/2002, NATO Grant No. PST.CLG.978953, the State of Florida, and the U.S. National Science Foundation.

- [1] M.V. Andrés, J. Gómez-Camacho, and M.A. Nagarajan, Nucl. Phys. **A579**, 273 (1994).
- [2] Y. Sakuragi, S. Funada, and Y. Hirabayashi, Nucl. Phys. **A588**, 65c (1995).
- [3] B. Buck and A.A. Pilt, Nucl. Phys. **A280**, 133 (1977).
- [4] M.V. Zhukov, B.V. Danilin, D.V. Fedorov, J.M. Bang, I.J. Thompson, and J.S. Vaagen, Phys. Rep. **231**, 151 (1993).
- [5] E.F. Aguilera, J.J. Kolata, F.D. Becchetti, P.A. DeYoung, J.D. Hinnefeld, A. Horvath, L.O. Lamm, Hye-Young Lee, D. Lizcano, E. Martinez-Quiroz, P. Mohr, T.W. O'Donnell, D.A. Roberts, and G. Rogachev, Phys. Rev. C **63**, 061603(R) (2001).
- [6] R. Raabe, A. Piechaczek, A. Andreyev, D. Baye, W. Bradfield-Smith, S. Cherubini, T. Davinson, A. Di Pietro, W. Galster, M. Huyse, A.M. Laird, J. McKenzie, W.F. Mueller, A. Ostrowski, A. Shotter, P. Van Duppen, and A. Wöhr, Phys. Lett. B **458**, 1 (1999).
- [7] R. Raabe, Ph.D. thesis, Katholieke Universiteit Leuven, Leuven, 2001.
- [8] H. Gemmeke, B. Deluigi, L. Lassen, and D. Scholz, Z. Phys. A **286**, 73 (1978).
- [9] N. Keeley, K.W. Kemper, and K. Rusek, Phys. Rev. C **66**, 044605 (2002).
- [10] G.R. Kelly, N.J. Davis, R.P. Ward, B.R. Fulton, G. Tungate, N. Keeley, K. Rusek, E.E. Bartosz, P.D. Cathers, D.D. Caussyn, T.L. Drummer, and K.W. Kemper, Phys. Rev. C **63**, 024601 (2001).
- [11] K. Rusek, K.W. Kemper, and R. Wolski, Phys. Rev. C **64**, 044602 (2001).
- [12] I.J. Thompson, Comput. Phys. Rep. **7**, 167 (1988).
- [13] J. Wang, A. Galonsky, J.J. Kruse, E. Tryggestad, R.H. White-Stevens, P.D. Zecher, Y. Iwata, K. Ieki, A. Horvath, F. Deak, A. Kiss, Z. Seres, J.J. Kolata, J. von Schwarzenberg, R.E. Warner, and H. Schelin, Phys. Rev. C **65**, 034306 (2002).
- [14] R.E. Warner, M.H. McKinnon, N.C. Shaner, F.D. Becchetti, A. Nadasen, D.A. Roberts, J.A. Brown, A. Galonsky, J.J. Kolata, R.M. Ronningen, M. Steiner, and K. Subotic, Phys. Rev. C **62**, 024608 (2000).
- [15] Y. Sakuragi, Phys. Rev. C **35**, 2161 (1987).
- [16] C.H. Dasso and A. Vitturi, Phys. Rev. C **50**, R12 (1994).
- [17] M. Dasgupta, D.J. Hinde, K. Hagino, S.B. Moraes, P.R.S. Gomes, R.M. Anjos, R.D. Butt, A.C. Berriman, N. Carlin, C.R. Morton, J.O. Newton, and A. Szanto de Toledo, Phys. Rev. C **66**, 041602 (2002).
- [18] J.J. Kolata, V. Guimaraes, D. Peterson, P. Santi, R. White-Stevens, P.A. DeYoung, G.F. Peaslee, B. Hughey, B. Atalla, M. Kern, P.L. Jolivet, J.A. Zimmerman, M.Y. Lee, F.D. Becchetti, E.F. Aguilera, E. Martinez-Quiroz, and J.D. Hinnefeld, Phys. Rev. Lett. **81**, 4580 (1998).
- [19] M. Trotta, J.L. Sida, N. Alamanos, A. Andreyev, F. Auger, D.L. Balabanski, C. Borcea, N. Coulier, A. Drouart, D.J.C. Durand, G. Georgiev, A. Gillibert, J.D. Hinnefeld, M. Huyse, C. Jouanne, V. Lapoux, A. Lépine, A. Lumbroso, F. Marie, A. Musumarra, G. Neyens, S. Ottini, R. Raabe, S. Ternier, P. Van Duppen, K. Vyvey, C. Volant, and R. Wolski, Phys. Rev. Lett. **84**, 2342 (2000).